https://journal.utripoli.edu.ly/index.php/Alqalam/index eISSN 2707-7179

Original article

Synthesis, Characterization, Antimicrobial Activity, DFT, Molecular Docking, and ADMET of 4-Chlorophenyazolquniolin-8-ol and Its Metal Complexes

Najla Abduljalil[1], Saleh Bufarwa[2*], Mustapha Belaidi[3], Reem El-Seifat[4], Abdulsalam Saleh[5], Marei El-ajaily[6]

[1]*Libyan Authority for Scientific Research, El-Beida, Libya*
[2]*Department of Chemistry, Faculty of Science, University of Omar Al-Mukhtar University, El-Beida, Libya*
[3]*Chemistry, Laboratory Environment and Sustainable Department, Ahmed Zabana University, Relizane, Algeria*
[4]*Natural Resources and Environmental Sciences, University of Omar Al-Mukhtar University, El-Beida, Libya*
[5]*Department of Health Food Hygiene, Omar AL Mukhtar University, EL-Beida, Libya*
[6]*Department of Chemistry, Faculty of Science, University of Benghazi, Benghazi, Libya*

ARTICLE INFO

Corresponding Email. *Saleh.bufarwa@omu.edu.ly*

Received*: 28-05-2024*
Accepted*: 16-07-2024*
Published*: 23-07-2024*

Keywords*. 8-Hydroxyquinoline, Mass Spectrometry, Antimicrobial Activity, Alzheimer's Disease, Molecular Docking.*

ABSTRACT

In this study, we prepared 4-chlorophenylazoquinoline, a derivative of 8-hydroxyquinoline, with Mn(II), Co(II), Ni(II), Cu(II), and Zn(II) ions to create metal complexes. We used various physical and spectroscopic methods to characterize the compound and its metal complexes, including molar conductivity measurements, melting point analysis, elemental analysis, electronic absorption spectroscopy, mass spectrometry, magnetic resonance spectroscopy, infrared spectroscopy, and thermogravimetric analysis. The octahedral geometry of all prepared complexes has been confirmed. To assess the antimicrobial activity, we examined two types of bacterial strains and two types of fungal strains. The antimicrobial activity of the prepared compounds was observed, and the higher increase was observed in the copper complex. The compounds were studied computationally after optimizing the angles, lengths, and bonds using the basic set 6-31G(d,p)/LANL2DZ. The molecular docking study of the compounds with the Alzheimer's disease protein 4BDT showed significant activity in binding to the amino acids of HL, C1, C2, C3, C4, and C5 compounds, with affinity energies of -6.4, -6.9, -6.9, -6.7, and -7.2 kcal.mol^{-1} for the compounds, respectively. To evaluate the safety of the prepared compounds in different drug designs, we employed the ADMET study, reducing the risk of failure in advanced drug design stages. The results of the ADMET showed a relative decrease in the toxicity and carcinogenicity factor. However, there are indications of metabolic risk and cellular uptake, requiring further study.

Cite this article. *Abduljalil N, Bufarwa S, Belaidi M, El-Seifat R, Saleh A, El-ajaily M. Synthesis, Characterization, Antimicrobial Activity, DFT, Molecular Docking, and ADMET of 4-Chlorophenyazolquniolin-8-ol and Its Metal Complexes. Alq J Med App Sci. 2024;7(3):*566-582. *https://doi.org/10.54361/ajmas.247320*

INTRODUCTION

Various structures in medical literature are defined by a chemical composition with multiple binding properties [1,2]. These structures can offer potent and precise ligands for various biological targets by altering the makeup of functional groups or incorporating specific groups [3]. The field of drug discovery and development has seen numerous published papers focusing on the identification of diverse and heterogeneous structures with biological significance [4,5]. One important heterogeneous compound that has garnered significant attention as a versatile drug is 8-hydroxyquinoline, the

most widely utilized quinoline in medical applications, which acts as an excellent scaffold group by forming chelation complexes with metal ions. 8-hydroxyquinoline is known for its antimicrobial properties and has a variety of other medical uses, including the treatment of neurodegenerative diseases and herpes. Ketolidinyl halogens are antiamoebic, have antifungal properties, and have been widely used to treat intestinal infections. One notable compound is clioquinol, which has been utilized in treating diarrhea for 30 years. It is undergoing phase II trials for the treatment of Alzheimer's disease. While there are potentially effective chemical treatments, the overuse and misuse of antibiotics have led to their ineffectiveness against certain bacteria. Consequently, researchers are exploring alternative compounds as potential antibiotics [5]. Azo dyes are utilized in industries such as textiles, paints, and foams, and have also demonstrated effectiveness in various biological applications [6,7]. Specifically, they have shown promise as solar cells [8], catalysts [9], robust corrosion gurd [10], removal of heavy elements from the aquatic medium [11], antimicrobial [12], antifungal [13], antioxidant, and cytotoxic agents [14]. Currently, their compounds are being examined for their potential as agents against pathogens. In this study, we synthesized a chlorine-containing azo derivative of 8-hydroxyquinoline and characterized the compound and its metal complexes using various physical and spectroscopic methods. Antimicrobial and antioxidant activities were conducted for the compounds and compared with some standard drugs. Additionally, we conducted computational studies on the compound and its complexes, optimizing angle lengths, bonds, energy calculations, and quantitative parameters. Furthermore, molecular docking of the compounds with a bacterial protein was performed to compare the experimental results with the theoretical findings.

METHODS

Chemicals

All chemicals used are of high purity and analytical grade, including manganese (II) chloride ($MnCl_2$. $4H_2O$; %98; Aldrich); Cobalt chloride ($CoCl_2.5H_2O$; %97; Aldrich), nickel chloride ($NiCl_2.5H_2O$; %98; Aldrich), copper(II) chloride ($CuCl_2.5H_2O$; %99; Aldrich), zinc chloride ($ZnCl_2$; %98; Aldrich), 8-hydroxyquinoline (C_9H_7NO; %98.5; Aldrich), p-chloroaniline ($C_6H_4NH_2Cl$; %98; Aldrich).

Appearance

The following methods were used in the experiments: Magnetic susceptibility calculations were performed at room temperature using the Faraday method (Faraday balance). Molar conductivity measurements of the compounds were obtained in dimethyl formaldehyde (DMF) solution at room temperature using a Jenway 4510 conductivity meter. Elemental analysis was conducted using a Perkin-Elmer 2400 CHN analyzer. Metal content was determined using a Thermo Scientific iCE 3300 atomic absorption spectrometer with an autosampler. FT-IR spectra were recorded using a Thermo Scientific 6700 and a KBr disk. Electronic spectra were obtained using a Beckman Coulter DU 800 spectrometer with dimethyl sulfoxide (DMSO) as the solvent. Mass spectra of the compounds were performed by a direct input unit (DI-50) with a Shimadzu QP-5050 GC-MS. ^{1}H NMR spectra were recorded using a Bruker Avance III high-performance NMR spectrometer at 400 MHz, with DMSO-d_6 as the solvent. ESR spectra of the powder complexes were recorded at room temperature using a Jeol JES-FE 2XG spectrometer. Most of the analyses were conducted by the microanalysis team at Cairo University, Giza, Egypt.

Biological assays for antimicrobial and antioxidant activity were performed at the Department of Microbiology, Omar Al-Mukhtar University. Anti-tuberculosis activity was evaluated at the Faculty of Veterinary Medicine in collaboration with the Animal Health Center in the Preventive Medicine and Public Health Laboratory.

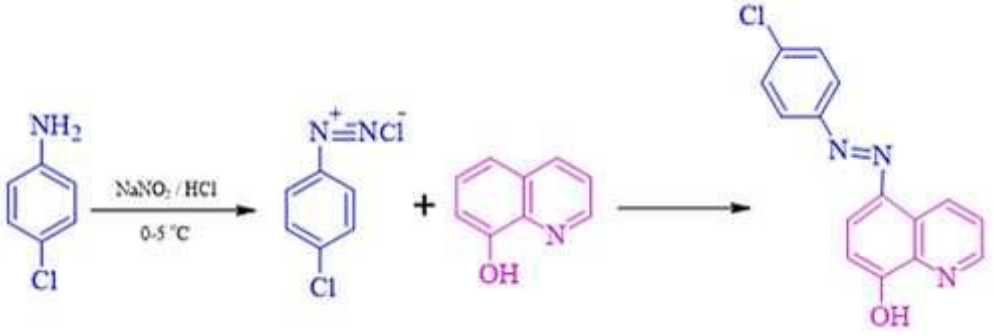

Figure 1. Preparation of 4-chlorophenylazoqinulinol-8-ol.

Synthesis

Synthesis of 5-(p-chlorophenylazo) quinoline

A solution containing 13.3 mmol of 5-chloroaniline in 40 ml of ethanol and 20 ml of 2 M HCl was cooled in an ice salt bath. It was azotized with (20 ml, 10.73 mmol) of sodium nitrite solution. The cooled diazonium solution was slowly added to a solution containing (1.55g, 10.73 mmol) g of 8-hydroxyquinoline while continuously stirring in 100ml ethanol and 602 mg potassium hydroxide. The product was recrystallized in ethanol multiple times [14,15].

Synthesis of solid complexes

The complexes were prepared by mixing a hot, saturated alcohol solution containing 0.001 mole of a metal ion dissolved in hot ethanol, mixed with the required amount of the investigated ligand (0.001 mmol), and forming 1:1 complex (16). The pH of the solution was kept at 6.5-7.5 by adding (1:10) a dilute ammonia solution. The reaction mixture was heated in a steam bath with occasional stirring for 4 hr, and then evaporated to dryness. The resulting complexes were recrystallized in ethanol. It was then filtered by suction, washed with ethanol until a colorless filtrate was obtained, suction-filtered, and finally kept in a vacuum desiccator [14,15].

Biological activity

Antimicrobial activity

The compounds' efficacy for antimicrobial activity was tested using the agar diffusion method (16, 17). Under identical concentrations and conditions, the compounds were compared with standard drugs such as ciprofloxacin, tetracycline, and amphotericin. The antimicrobial activity was evaluated against *B. subtilis*, S. aureus, *E. coli*, and *P. aeruginosa* (Gram-negative) strains, as well as two strains of fungi, *A. flavus* and *C. albicans* [18].

Computational studies

The computational studies mentioned below were conducted on the organo-complex and its active anti-tuberculosis metal complexes to support and corroborate the in vitro findings.

Generation and optimization of compounds

The molecular editor GaussView 6.0 was utilized to generate and optimize the three-dimensional structure of the organic ligand and its metal complexes. To obtain the optimization of exchange and correlation functions, B3LYP was employed with the basic set 6-31G(d,p)/LANL2DZ.

Obtaining the three-dimensional structure of the target

The target structure for pfndh was obtained from the Protein Data Bank (PDB) (www.rcsb.org) to serve as the intended target.

Molecular Docking

The importance of molecular docking lies in its ability to predict how compounds will fit into the active sites of target molecules, as well as to foresee the binding aspects of specific interactions. Using the AutoDock tool [19], we conducted molecular docking on an organic ligand and its complexes with a specific target of the Mycobacterium tuberculosis structure (PDB ID: 4BDT) obtained from the Protein Data Bank.

DFT analysis

The analysis of molecular properties and chemical reactions to predict how compounds interact is mostly done using theoretical methods. These methods are commonly used to determine the molecular structure of synthesized compounds because they are efficient and accurate. As a result, some theoretical studies have been conducted to gather more information on the computational calculations of prepared compounds. Related areas have also been studied using density functional theory (DFT). The study of the relationship between geometry and electronic properties of chemical compounds, including the highest occupied molecular orbitals (HOMO) and lowest unoccupied molecular orbitals (LUMO), is crucial, as well as some quantitative parameters. Additionally, the bond lengths and angles of prepared compounds have been calculated computationally [20,21].

ADMET Analysis

The AdmetSAR web server was used to predict the absorption, metabolism, and carcinogenicity of the ligand and its metal complexes. The structures of the compounds were uploaded to the server and drug-like compounds were evaluated based on their ADMET properties.

RESULTS AND DISCUSSION

Chemistry

Metal complexes of Mn(II), Co(II), Ni(II), Cu(II), and Zn(II) were prepared in the solid state. They are soluble in some organic solvents, such as DMF and DMSO, but insoluble in water [22]. The low molar conductivities of the compounds were measured in 10^{-3} M DMF solution at room temperature, indicating that they are nonelectrolytes. The thermal stability of the compounds up to 253 °C was determined by TGA. The octahedral geometry of the N and O atoms of the quinoline ligand in the compounds was determined using different spectroscopic methods [15,23].

Table 1. Physical features of ligand (HL) along with its complexes

Compound	Molecular Formula	M.wt	Color	Yield%	Λ_m	μeff	M.p °C	(Cal.) Found%			
								C	H	N	M
HL	$C_{15}H_{10}NOCl$	283	Orange	83	-	-	132	(63.40) 63.99	(3.87) 4.15	(14.79) 14.27	- -
C1	$C_{15}H_{16}N_3MnO_5Cl$	408.7	Brown	72	6.2	5.91	184	(42.30) 42.64	(3.99) 3.89	(9.87) 9.43	(12.91) 12.76
C2	$C_{15}H_{15}N_3CoO_4Cl_2$	431	Brown	79	6.2	3.07	188	(40.45) 39.69	(3.82) 3.67	(9.43) 9.46	(13.24) 13.43
C3	$C_{15}H_{15}N_3NiO_4Cl_2$	430.8	Red	78	6.2	2.03	174	(48.49) 48.98	(4.58) 4.21	(11.31) 11.45	(15.81) 15.65
C4	$C_{15}H_{16}N_3CuO_5Cl_2$	417.3	Brown	76	6.2	1.33	181	(43.05) 43.34	(4.00) 4.09	(10.00) 10.16	(15.20) 15.14
C5	$C_{15}H_{16}N_3ZnO_5Cl_2$	419.9	Orange	75	6.2	0.00	195	(42.86) 42.34	(4.04) 4.22	(10.00) 9.84	(15.57) 15.42

Mass Spectra

The mass spectrometry of the substituent ligand and its complexes was performed at 70 eV at 220 °C, Figure 2 shows the mass spectra of the organic ligand. The results showed that the HL, C1, C2, C3, C4, and C5 had mass spectra at 281, 405.8, 430.6, 428, 415.9, and 417.5 respectively.

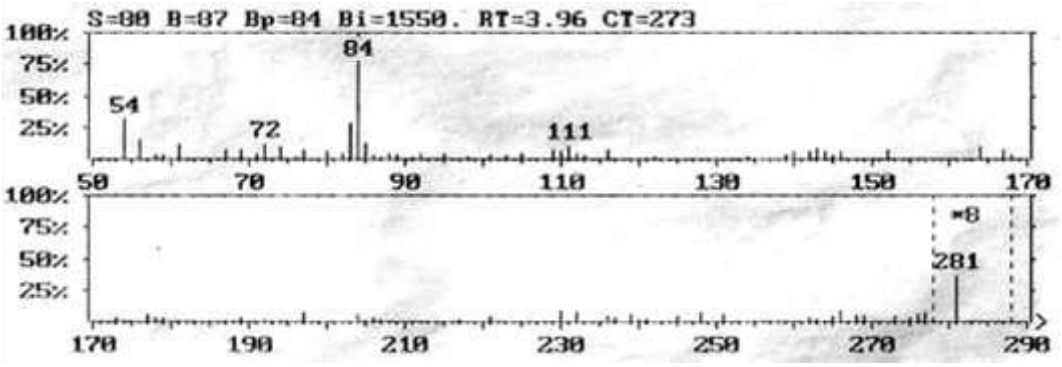

Figure 2. This is a figure. Schemes follow the same formatting.

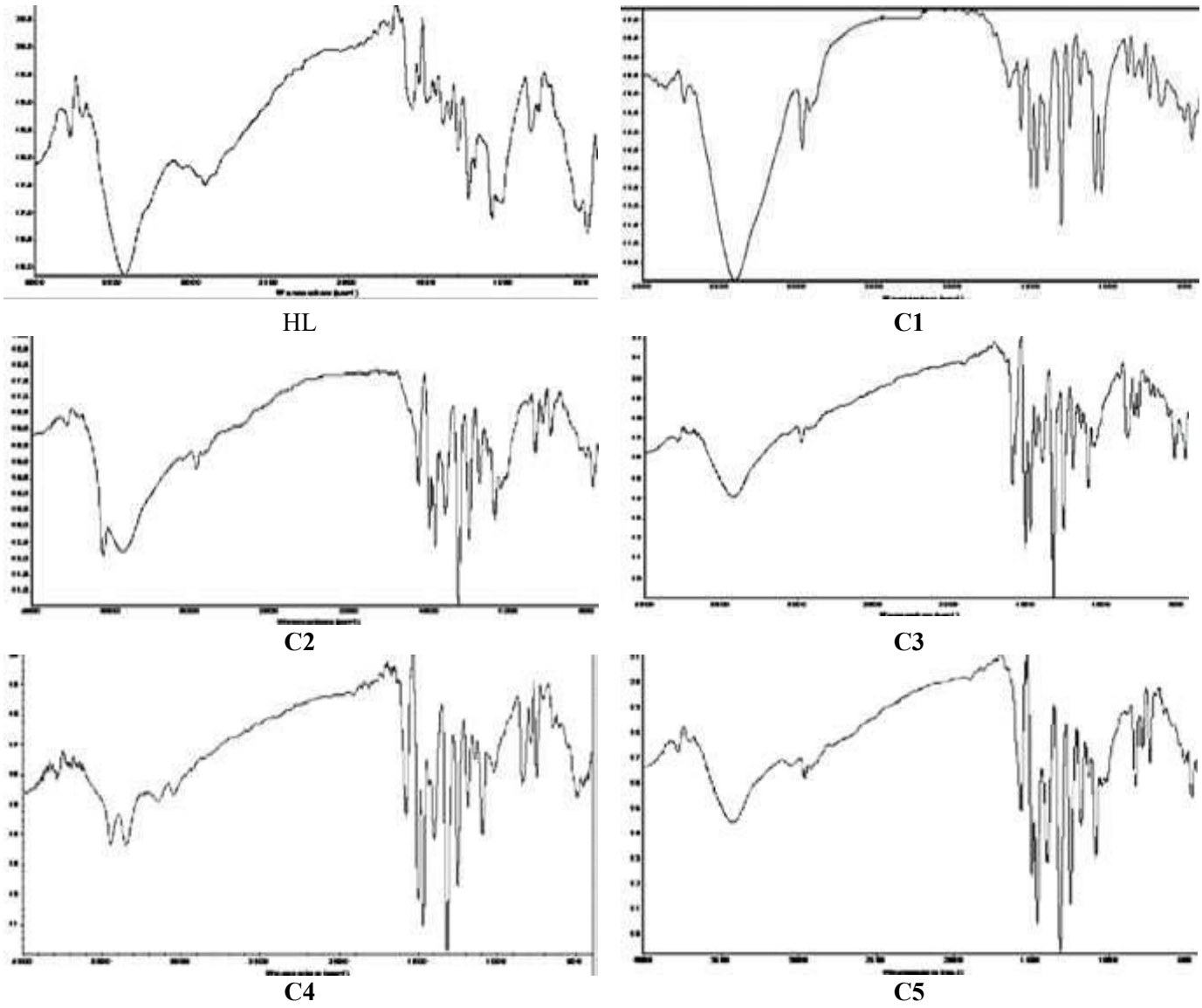

Figure 3. FT-IR spectra of ligand and its complexes.

FT-IR spectra

Absorption bands of azoquinoline derivatives have been reported in previous studies. Moreover, the stretching of CO and the deformation of OH lead to strong absorption bands in the low-frequency region. In the infrared spectra of the complexes (Table 2, figure 3), the band observed at 1404 cm^{-1} assigned to νN=N in the free ligand (HL) shows no shift upon complex formation, indicating that it is not a center of chelation. In the complexes, a band was observed within the range 3133-3448 assigned to the vO–H of coordinated water and water of hydration. For the C1 and C4 complexes, broadband appeared at 3547 and 3443 cm^{-1} respectively, corresponding to the OH- of neutralization. The observed bands at 1565-1586 cm^{-1} for vC=N, 1460-1467 cm^{-1} for vC=C, and 1236-1256 cm^{-1} for vC-O are shifted to lower wave numbers due to complexes, indicating that it is a center of chelation. The metal complexes' spectra show bands ranging from 505–586 and 409–480 cm^{-1}, which are likely due to the stretching frequencies of (M→N) and (M–O) bonds, respectively. In simpler terms, these bands likely come from the coordination and covalent bonding between the donor atoms N and O and the central metal ion [24,25].

Table 2. Characterization of the infrared spectra of the ligand and its complexes.

	$OH_{phenlic}$	$OH_{coordnate}$	C=C	C=N	N=N	M-N	M-O
HL	3366	-	1461	1577	1404	-	-
C1	-	3420	1465	1573	1401	524	461
C2	-	3312	1462	1573	1401	529	464
C3	-	3422	1465	1578	1400	525	455
C4	-	3444	1460	1582	1400	504	444
C5	-	3419	1466	1571	1403	517	463

^{1}HNMR spectra

The ^{1}H NMR spectra of the ligand exhibit a singlet signal at (3.37) ppm which is assigned to the CH_3 protons of the solvent. The signals observed in Figure 4 at 6.95–6.67 ppm is assigned to the protons of the pyridine ring and those observed at 8.92-7.07 ppm are assigned to the protons of the aromatic ring. For Zn-L (C5) complexes in Figure 5, the single peak observed at 9.44 ppm in the free ligand corresponding to the OH group disappeared due to complexation. This resulted in the appearance of a new signal in the region of 3.61 and 3.48 ppm, corresponding to coordinated water molecules for the **C5**, respectively. All other signals observed in the free ligand are still present with some up-field shift, which may be due to complexation. Table 2 shows the ^{1}H NMR spectra data for the HL and C5.

Table 3. This is a table. ^{1}H NMR data in ppm for the organic ligand and its zinc complex

Compound	^{1}HNMR (DMSO-d_6- 300 MHZ)
HL	δ 9.44 OH, δ 9.03 -7.56 Aromatic C-H protons, δ 7.43-7.28 Pyrdine ring C-H, δ 3.66 H_2O solvent protons, δ 2.50 DMSO protons
C5	δ 8.78 -7.56 Aromatic C-H protons, δ 6.89 -6.85 Pyrdine ring C-H, δ 3.61H_2O of coordination, δ 2.51DMSO protons

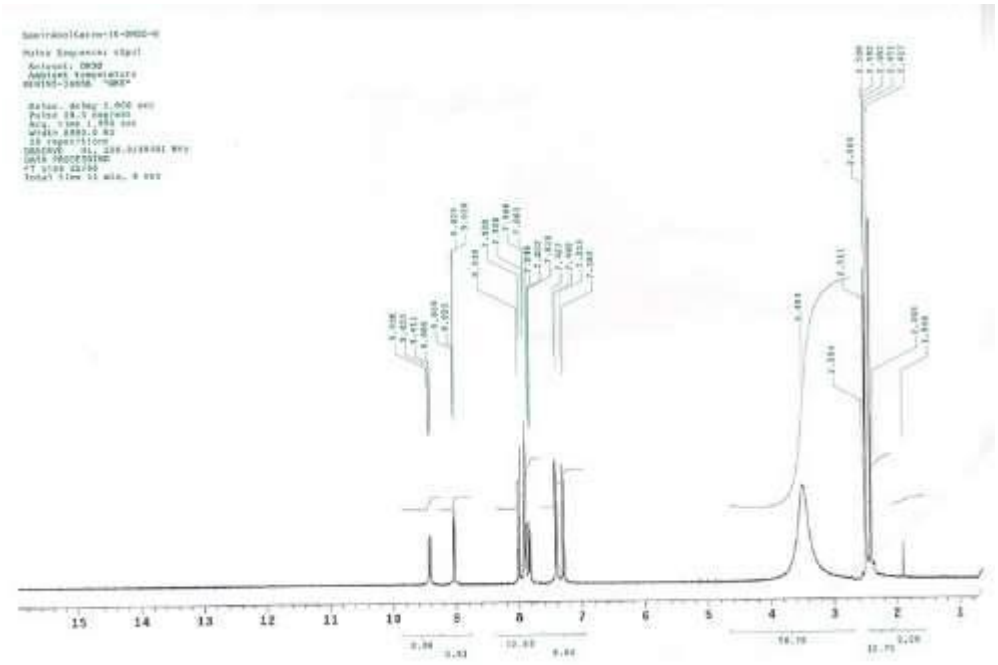

Figure 4. ^{1}H NMR spectra of ligand (HL).

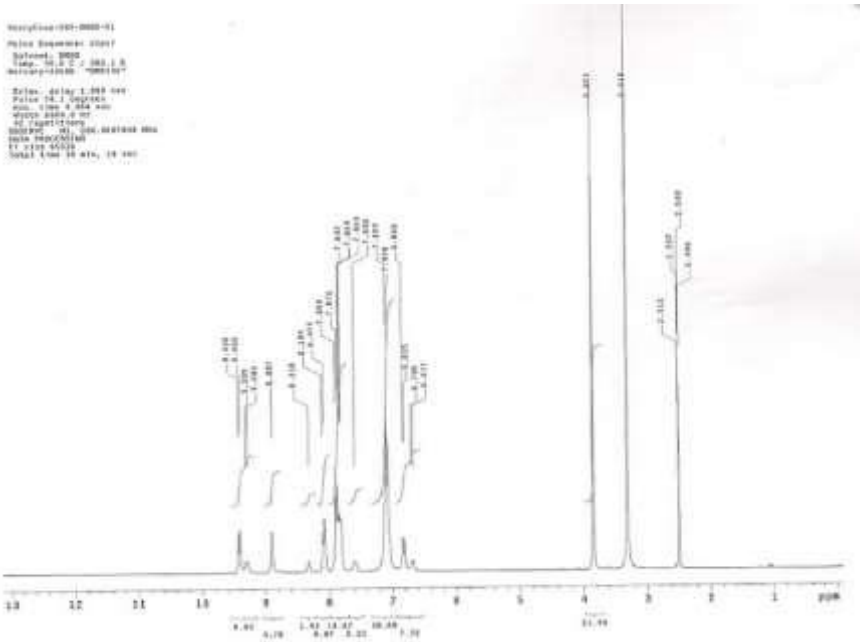

Figure 5. ^{1}H NMR spectra of C5

Electronic absorption and magnetic moment

The electronic absorption spectra of the investigated ligand (HL), as shown in Figure 6, exhibit two bands at 380 nm (26316 cm^{-1}) and 390 nm (25641 cm^{-1}). The first band may be assigned to the π-π* transition within the phenyl moiety,(26) and the second band may be ascribed to the n-π* transitions within the -N=N- followed by intramolecular charge (C.T.) or interligand transitions within the ligand. The electronic absorption spectra of the divalent Cu metal ions with the investigated ligand complex (C4) are displayed in Figure 6. These spectra show two absorption bands at 220 nm (45454 cm^{-1}), 380 nm (26316 cm^{-1}), and a shoulder at 470 nm (21276 cm^{-1}). These bands can be attributed to charge transfer $^{2}A_{2g} \rightarrow {}^{2}T_{1g}$ transitions. It was suggested that an octahedral configuration exists around the central metal ion [20, 27].

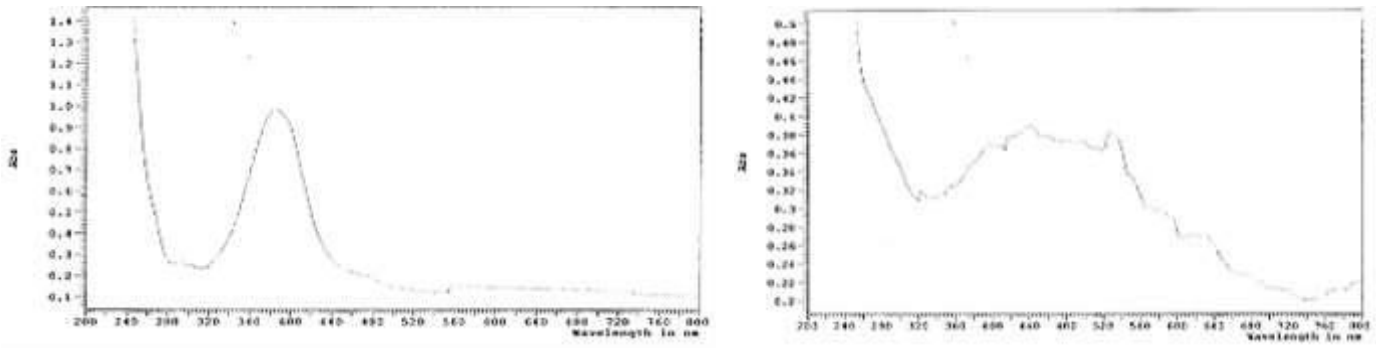

HL **C4**

Figure 6. This is a figure. Schemes follow the same formatting.

TGA and DTA studies

The TGA and DTA analysis methods offer more opportunities for screening metal complexes [28]. This study aims to gather information on the thermal stability of divalent transition metal complexes (5-(p-chlorophenylazoquinolin-8-ol), determine the position of water molecules (if present) as either inner or outer sphere, and propose a general scheme for the thermal decomposition of these complexes. The thermogram shows a decrease in sample weight with a simultaneous linear increase in temperature. In this study, heating rates were controlled at 10 °C/min, and weight loss was observed up to 1000 °C. The weight loss of each complex was calculated based on TG curves (Figure 7), and the results are recorded in Table 4, taking into account the proposed stoichiometry. The TG curves illustrate the decomposition of the organic part of the chelated complexes. This process continues until a constant weight is reached, at which point metal oxide (MO) residues are formed as the final product of the complexes. In the [Mn-L4] (C1)] complex, the only water

molecule was ejected within the temperature range of 99-110 °C, resulting in a weight loss of 4.53% (Calculated: 4.23%). Then, in the temperature range of 110-301 °C, a weight loss of 63.02% (calculated: 64.00%) was observed, which corresponds to the loss of two phenyl groups, three carbon atoms, one chloride atom, and two oxygen atoms. Finally, in the temperature range of 301-564 °C, a weight loss of 17.23% (calculated: 17.39%) was observed, which corresponds to the loss of three nitrogen atoms and two oxygen atoms. The metal content at the end of the thermogram was calculated from the remaining metal oxide and was found to be 16.45% (calculated: 16.67%). In the case of the C1, the DTA curve shows an endothermic peak at 196 °C, indicating the removal of the hydration water. There are also two exothermic peaks on the DTA curve at 460 °C, corresponding to the removal of the coordinated water, and at 631 °C, indicating the decomposition of the organic matter and the formation of an intermediate species, followed by the rearrangement of the decomposed species. When the temperature rises above 631 °C, combustion occurs, followed by the removal of carbon from the organic matter, leaving behind a metal residue such as MnO.

Table 4. Tg and DTA analysis of the decomposition of C1

Complex (ligand-metal)	M.wt	Temp (°C)	Caltd loss%	Found loss%	Assignment
C1	425.5	99-110	4.23	4.53	H_2O
		110-301	64.00	63.02	$C_{15}H_{15}$-Cl-O_2
		301-564	17.39	17.23	N_3- O_2
		564-1063	16.67	16.45	MnO

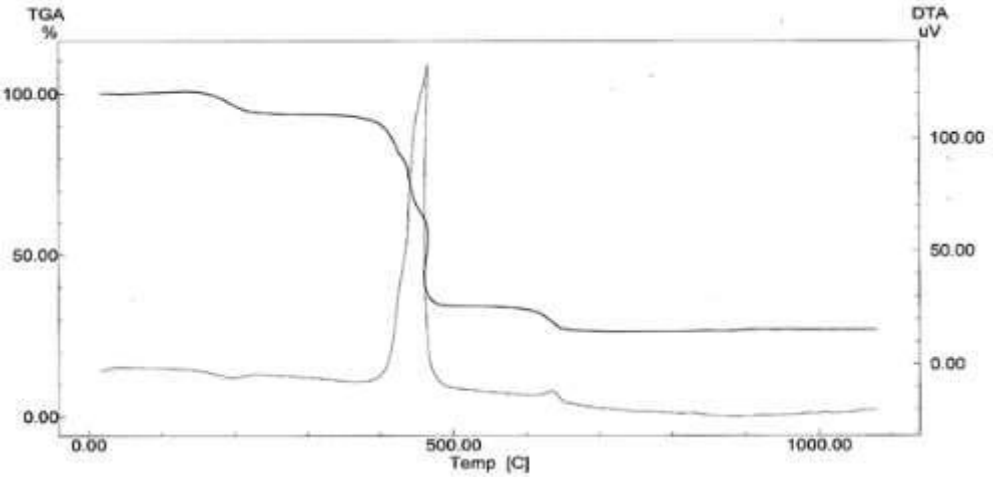

Figure 7. Thermogravimetric and differential thermal analysis curves of C1.

Computational studies

DFT analysis

The two main orbitals critical to chemical stability are the highest occupied molecular orbital (HOMO) and the lowest unoccupied molecular orbital (LUMO) [29]. The HOMO orbital can donate an electron, while the LUMO orbital can accept an electron. [16,30]. Table 5 and Figure 8 show the energies of the HOMO and LUMO orbitals obtained from the calculations of compounds C1, C2, and C3, along with additional parameters such as the HOMO-LUMO energy gap (Eg), absolute electronegativity (ϒ), chemical potential (Pi), absolute hardness (η), absolute softness (σ), overall electronegativity (ω), overall softness (S), and additional electronic charge (ΔN_{max}). The energy gap Eg is essential for predicting the stability of a compound, with a lower value indicating higher reactivity. Among the compounds, C3 was found to be the most reactive, with the energy gap values of C1, C2, C3, and C4 being 2.65, 2.86, 2.83, 2.45 and 3.04 eV, respectively [31].

Table 5. The calculated quantum chemical parameters of the complexes

Compound	HOMO	LUMO	Eg	χ	η	σ	Pi	S	ω	ΔN
C1	-5.03	-2.37	2.65	3.7	1.33	0.752	-3.7	0.376	5.146	2.78
C2	-5.43	-2.57	2.86	4	1.43	0.699	-4	0.349	5.594	2.79
C3	-5.69	-2.86	2.83	4.27	1.42	0.704	-4.27	0.352	6.419	3.01
C4	-5.86	-3.41	2.45	4.64	1.23	0.813	-4.64	0.406	8.752	3.77
C5	-5.41	-2.37	3.04	3.89	1.52	0.658	-3.89	0.328	4.976	2.56

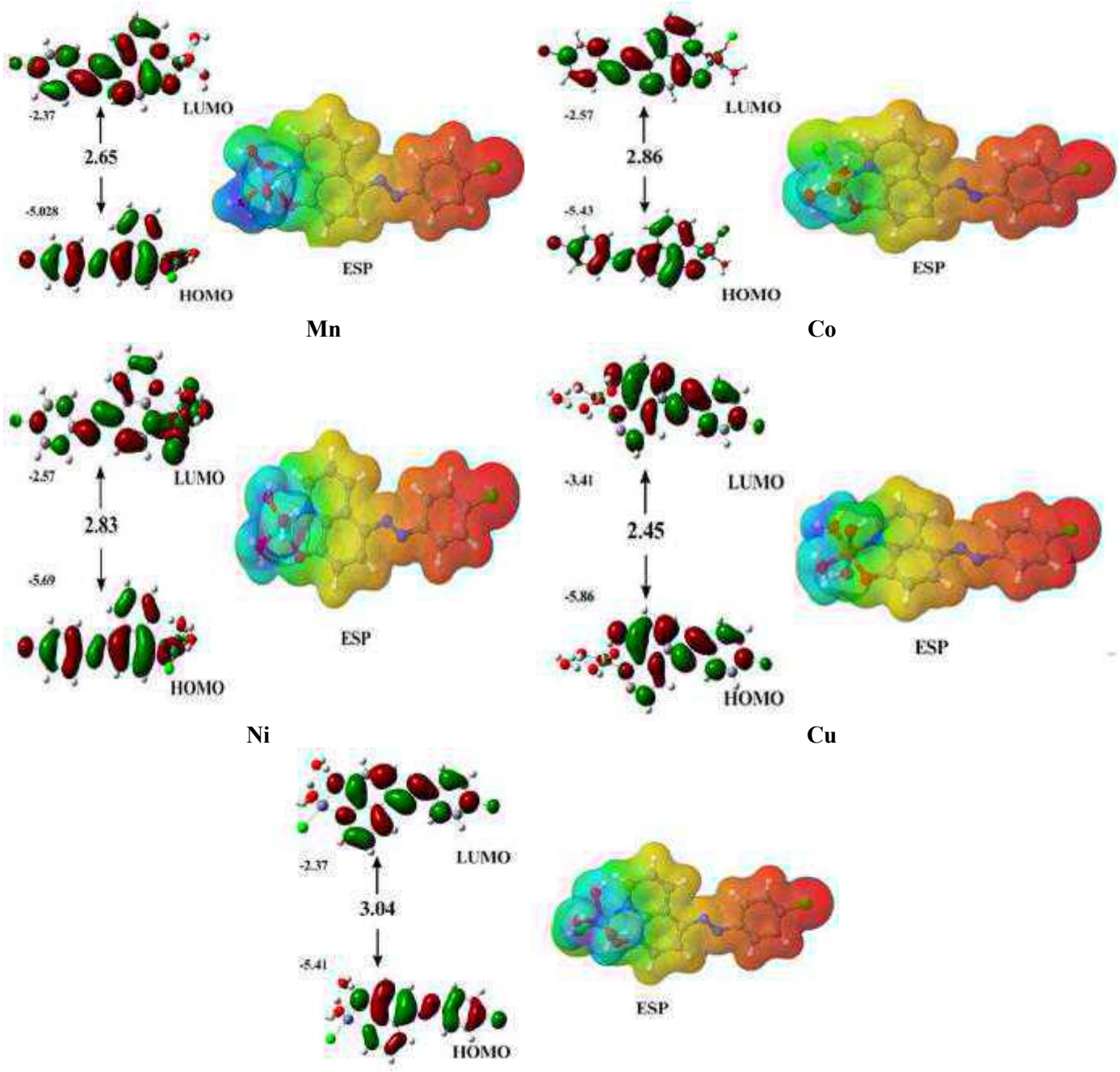

Figure 8. Molecular orbital distribution plots of HOMO, LUMO state, and MESP of the compounds

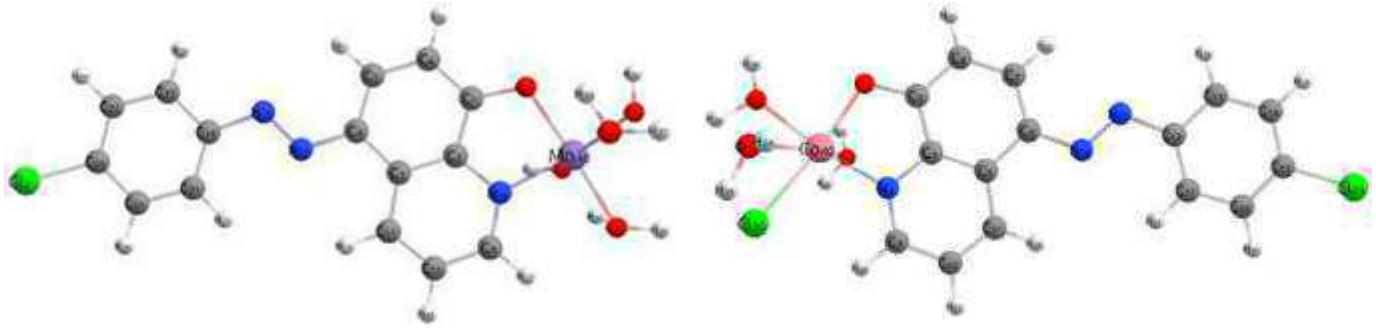

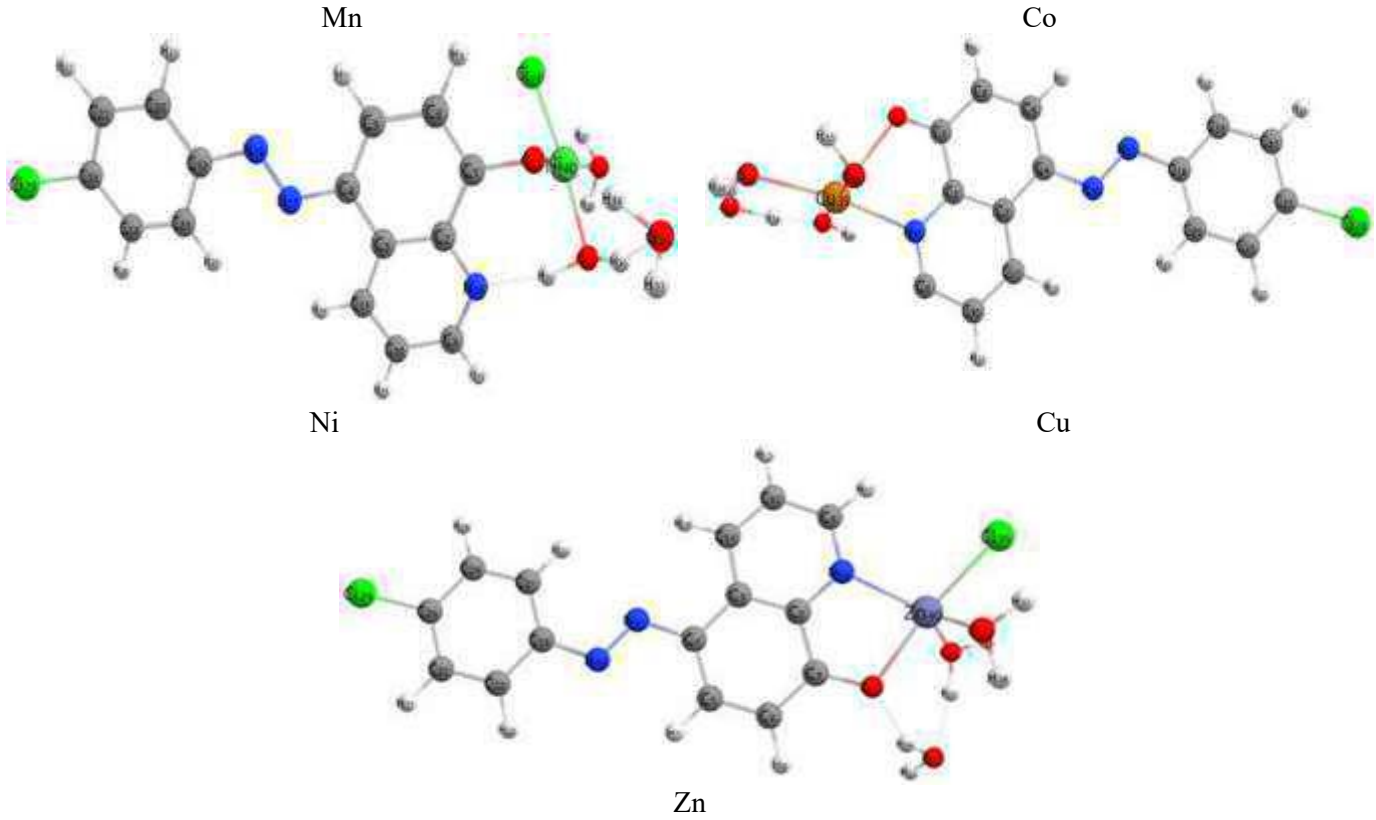

Figure 9. Optimization geometry of compounds

Table 6. The selected angle length (Aº) of complexes

C1		C2		C3		C4		C5	
C1-C2	1.443	O1-C3	1.33	C1-C2	1.445	C1-C2	1.479	C1-C2	1.45
C1-C6	1.414	O1-Co40	1.95	C1-C6	1.398	C1-C6	1.457	C2-N16	1.364
C1-O15	1.338	N2-C4	1.38	C1-O15	1.326	C1-O14	1.274	C4-N17	1.397
C2-C3	1.425	N2-Co40	1.96	C2-N16	1.367	C2-C3	1.419	O31-Zn40	2.101
C2-N16	1.385	C3-C4	1.45	C4-N17	1.403	C9-N15	1.299	O32-Zn40	2.176
C3-C4	1.441	C3-C8	1.41	C9-N16	1.322	O14-Cu39	2.519	C26-Cl29	1.757
C3-C11	1.429	C4-C5	1.42	O15-Ni40	1.854	N15-Cu39	2.128	O15-Zn40	2.09
O15-Mn40	2.002	C6-N28	1.41	N17-N18	1.266	N16-N17	1.319	N16-Zn40	2.122
N16-Mn40	1.991	C12-N27	1.43	N18-C19	1.412	N17-C18	1.41	N17-N18	1.268
N17-N18	1.3	C15-Cl29	1.82	C26-Cl29	1.755	C25-Cl28	1.812	-	-
N18-C19	1.427	N27-N28	1.3	O30-Ni40	1.941	O29-Cu39	1.922	-	-
C26-Cl29	1.823	Cl3-Co40	2.41	O32-Ni40	1.95	O31-Cu39	2.015		
O30-Mn40	2.077	O31-Co40	2.21	Cl39-Ni40	2.217	O32-Cu39	1.887	-	-
O31-Mn40	2.111	O33-Co40	2.28	-	-	-	-	-	-
O32-Mn40	2.108	O35-Co40	2.01	-	-	-	-	-	-
O33-Mn40	2.036	-	-	-	-	-	-	-	-

Molecular Docking

a molecular docking study was conducted using AutodockVina to simulate the docking of designed compounds as potential Alzheimer drugs with the target amino acids of the protein (PDB ID: 4BDT) (Figure 10). The study aimed to verify the binding properties of these compounds [32,33]. Table 7 summarizes the binding affinity and type of binding between the compounds and the active sites in the protein's amino acids. The study revealed that the compounds formed hydrophobic interactions via Pi-alkyl bonding with the major residues of the aromatic ring of the pyridine moiety. Additionally, Pi-anion binding was observed only in compound (C2), where it interacted electrostatically with amino acid through the aromatic ring of the pyridine moiety. Based on the binding affinity values, it was found that compound (C4) exhibited the highest binding capacity with the protein of target compared to the other compounds as shown by docking studies.

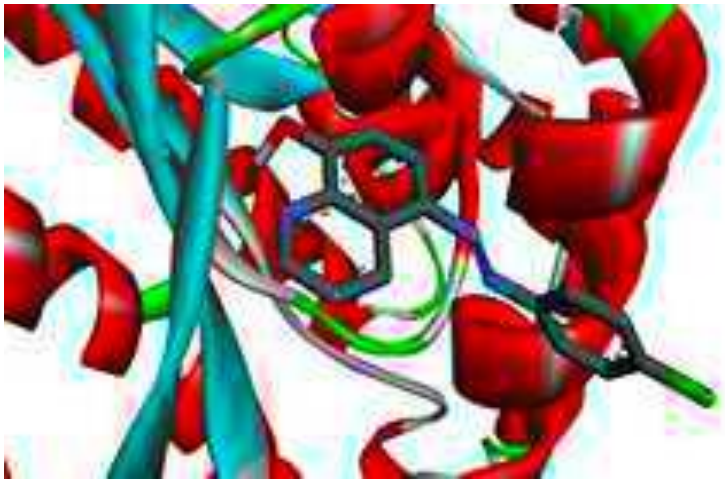

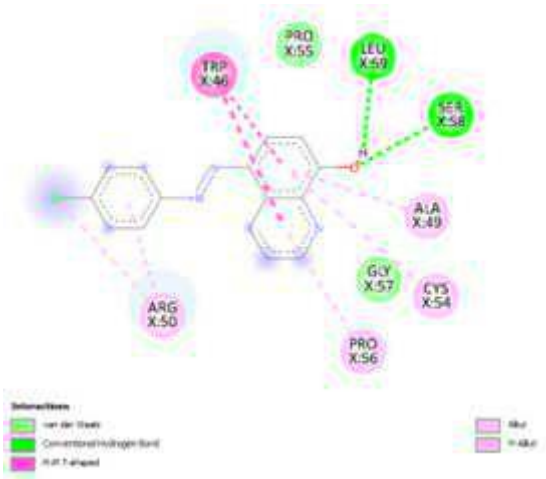
PRO X:55
LEU X:49
TRP X:46
SER X:58
ALA X:49
GLY X:57
CYS X:54
ARG X:50
PRO X:56

HL

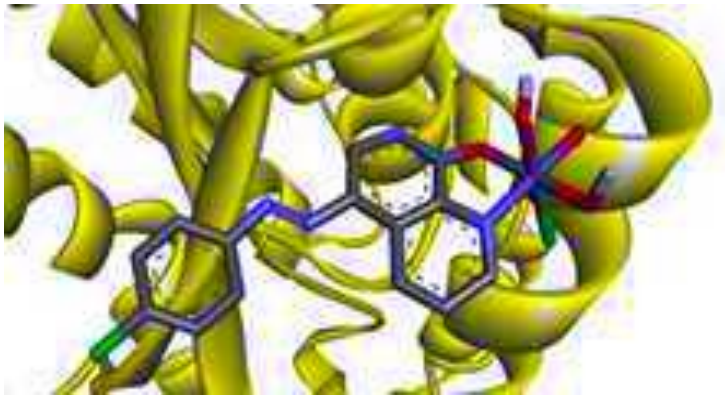

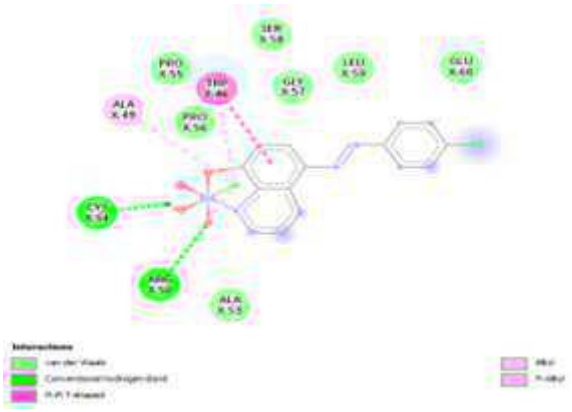

C1

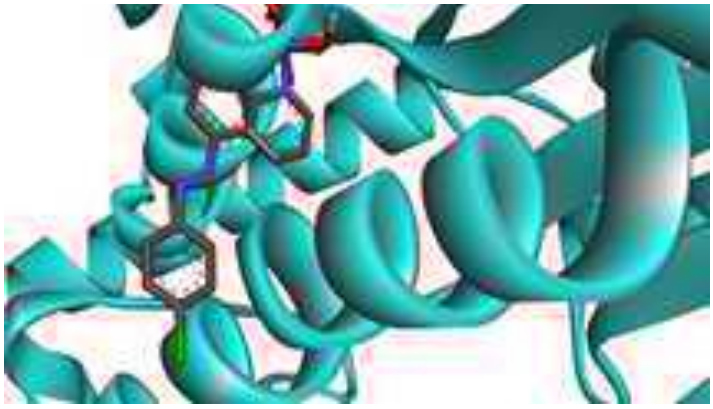

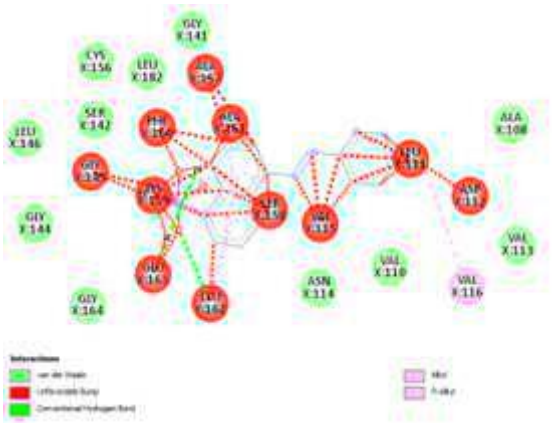
GLY X:141
CYS X:156
LEU X:182
SER X:142
LEU X:146
ALA X:108
GLY X:144
VAL X:113
ASN X:114
VAL X:116
GLY X:164

C2

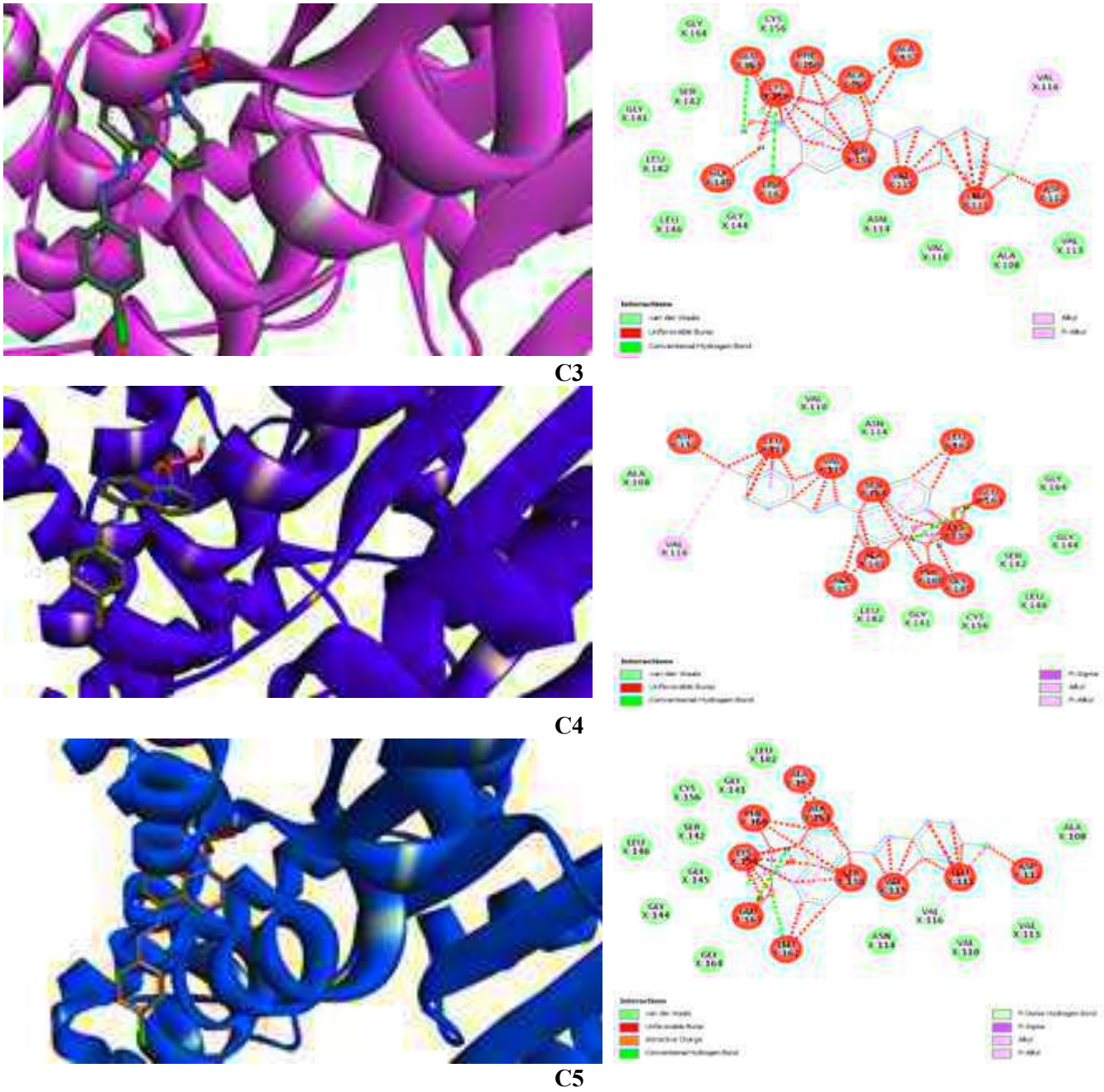

Figure 10. Predicted positions of the following molecules from docking analysis: (a) H2L; (b) C1; (c) C2; (d) C3; (e) C4, and their binding interactions with amino acids.

Table 7. Bonding affinity of compounds

Title 1	Bonding affinity
HL	-6.4
C1	-6.9
C2	-6.9
C3	-7.0
C4	-6.7
C5	-7.2

ADMET Studies

Many chemical compounds cannot be used as drugs for several reasons [34]. The most important of these reasons are insufficient absorption or distribution, high levels of toxicity, or excretion. All of these factors are known as ADMET.

To determine whether an organic compound and its manufactured metal complexes have a toxic effect, they must be carefully tested. The AdmetSAR web server calculated the ADMET parameters, including pharmacokinetic, pharmacodynamic, and human intestinal absorption parameters. Azoquinoline ligand and its metal complexes (II) show promising pharmacokinetic properties for human intestinal absorption (Table 8). Negative values indicate low P-glycoprotein and CYP2D9 inhibitory activity. The ligand and its metal complexes also show similar values for oral toxicity. Additionally, they are considered safer than some drugs that disrupt liver function because they show negative results for hepatotoxicity. Although the positive parameter values are moderate, they still pose a risk as a drug design.

Table 8. ADMET parameter of the ligand and its complexes

Compound	Model	Result	Probability
Absorption			
HL	Human Intestinal Absorption	HIA+	0.8920
C1	Human Intestinal Absorption	HIA+	0.8914
C2	Human Intestinal Absorption	HIA+	0.8915
C3	Human Intestinal Absorption	HIA+	0.8919
C4	Human Intestinal Absorption	HIA+	0.8920
C5	Human Intestinal Absorption	HIA+	0.8926
Distribution			
HL	Subcellular localization	Mitochondria	0.5382
C1	Subcellular localization	Mitochondria	0.5384
C2	Subcellular localization	Mitochondria	0.5387
C3	Subcellular localization	Mitochondria	0.5387
C4	Subcellular localization	Mitochondria	0.5387
C5	Subcellular localization	Mitochondria	0.5387
Metabolism			
HL	CYP450 2C9 Inhibitor	Non-inhibitor	0.7106
C1	CYP450 2C9 Inhibitor	Non-inhibitor	0.7104
C2	CYP450 2C9 Inhibitor	Non-inhibitor	0.7108
C3	CYP450 2C9 Inhibitor	Non-inhibitor	0.7103
C4	CYP450 2C9 Inhibitor	Non-inhibitor	0.7109
C5	CYP Inhibitory Promiscuity	Low CYP Inhibitory Promiscuity	0.8004
Toxicity			
HL	Acute Oral Toxicity	III	0.5664
	Carcinogenicity (Three-class)	Non-required	0.4843
C1	Acute Oral Toxicity	III	0.5666
	Carcinogenicity (Three-class)	Non-required	0.4844
C2	Acute Oral Toxicity	III	0.5667
	Carcinogenicity (Three-class)	Non-required	0.4843
C3	Acute Oral Toxicity	III	0.5661
	Carcinogenicity (Three-class)	Non-required	0.4843
C4	Acute Oral Toxicity	III	0.5668
	Carcinogenicity (Three-class)	Non-required	0.4848
C5	Acute Oral Toxicity	III	0.5663
	Carcinogenicity (Three-class)	Non-required	0.4848

Antimicrobial activity

The study tested compounds for their antibacterial and antifungal activities against six microorganisms, including *B. subtilis*, *S. aureus*, *E. coli*, *P. aeruginosa*, *A. flavus*, and *C. albicans* as shown in Table 5. The compounds showed moderate to good antibacterial activity compared to standard drugs. However, C3 showed more significant activity against *C. albicans*. The compounds also showed higher activity against bacterial strains, sometimes higher than standard drugs. This could be due to the chelation theory [35,36].

Table 9. Antimicrobial activity of the investigated complexes

Compound	*B. subtilis*	*S.aureus*	*A.flavus*	*C.albicans*
HL	30.8	4	12.5	6
C1	14.8	4	12.7	1.6
C2	14	6.9	17	9
C3	16.8	4.7	33.9	15.8
C4	17.6	4	3.9	14.7
C5	12	6	15.5	5
Tetracycline	2	1	2	2
Amphotericin B	1	4	1	15

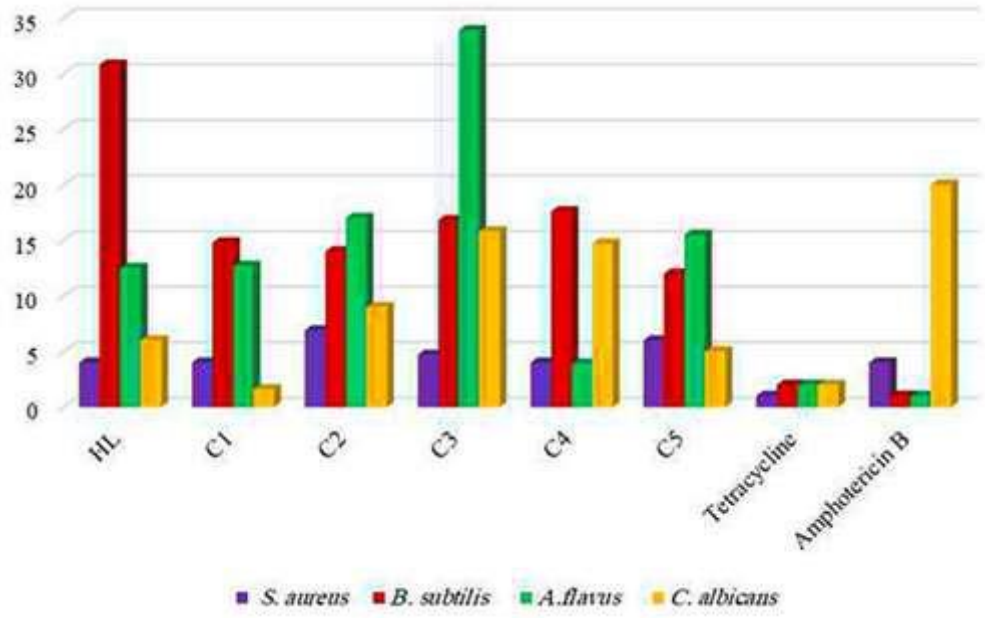

Figure 12. Antimicrobial activity of the compounds and standard drugs

CONCLUSION

The research involved the preparation and characterization of 4-chlorophenylazoquinoline and its metal complexes. Various analyses such as molar conductivity, elemental analysis, mass spectrometry, infrared, and thermal studies confirmed the octahedral geometry of the prepared complexes. Magnetic resonance spectroscopy data indicated the involvement of the phenolic hydroxyl group in the chelation process with the metal ion. The compounds were tested for antimicrobial activities and demonstrated effectiveness against the tested bacterial and fungal strains, outperforming some standard drugs. Molecular docking of the compounds with Alzheimer's disease protein showed promising affinity energy, indicating potential pharmacological effect. Additionally, the compounds were examined for their absorption, distribution, metabolism, excretion, and toxicity activities, suggesting potential pharmacological effects with some associated risks that warrant further investigation.

Acknowledgments

The authors would like to express their thanks and gratitude to their departments and Faculties.

Conflicts of Interest

The authors declare no conflicts of interest.

REFERENCES

1. Eldein S, Almabruk MI. Transitional Period Effects on Some Biochemical and Hormonal Parameters in Libyan Cows.
2. Abdelghani KA, Nisrin FK, Idress SMBA. Universal Journal of Chemistry and Applications.
3. Eltawaty SI, Omare M, Almagboul AZ, Tarig M, Mohammad A, Bofarwa SM. The Potential Antioxidant and Hepatotoxicity of Methanolic Extract of Leaves of Libyan capparis Spinosa Subsp Orientalis (duh.) Jafri in Rats. World J Pharm Res. 2018;7(5):101-12.

4. Mohamed S, Abdel-Latif SA, El-Ansary AL, Salim AI. Green Spectrophotometric Assessment for Molnupiravir Quantification in Pharmaceutical Formulations and Biological Fluids: Study of Structural Elucidation and Theoretical Approach. Egyptian Journal of Chemistry. 2024;67(7):513-24.
5. Mahmoud R, Mohamad NA, Saleh A, Bufarwa SM, Reem E-S. Exploring the effect of heat treatments on eliminating the remains of antibiotic residues (colistin). African Journal of Advanced Pure and Applied Sciences (AJAPAS). 2024:132-7.
6. Abbas OA, El-Roudi OM, Abdel-Latif SA. Novel 1, 3-diphenyl-4-(N, N-dimethylimido dicarbonimidic diamide azo)-5-pyrazolone and its chelates with manganese, nickel, copper, and zinc divalent metal ions as an antibacterial activity supported by molecular docking studies: Design, synthesis, DFT, and TD-DFT/PCM calculations. Applied Organometallic Chemistry. 2023;37(10):e7236.
7. Abdel-Kader NS, Abdel-Latif SA, El-Ansary AL, Hemeda MA. Design, synthesis, spectroscopic studies, DFT, TD-DFT/PCM calculations, and molecular docking studies on the anti-SARS and anti-COVID-19 activities of novel benzidine bis azo 1-(2-hydroxy-3-naphthoic acid) complexes with some transition metal ions. Polycyclic Aromatic Compounds. 2023:1-32.
8. Taher SE, Bofarwab SM. Study of Photonic and Electrochemical Properties of New Electroactive Material.
9. Elmanfe G, Bofarwa SM. Ceria catalyst promoted with Al 3+ and acidified with PO4 3-i) synthesis and surface textural properties. Am J Mater Sci. 2015;5:10-5.
10. Fadl A, Sadeek S, Magdy L, Abdou M. Robust corrosion guard, mechanical and UV aging properties of metal complex/epoxy hybrid composite coating for C-steel applications. Scientific Reports. 2022;12(1):12483.
11. Yaghi MM, Bufarwa SM, El Ziani NO. Analysis of some Heavy metals in baby food of pureed fruit available in the Libyan markets.
12. Al-Resayes SI, Jarad AJ, Al-Zinkee JM, Al-Noor TH, El-ajaily MM, Abdalla M, et al. Synthesis, characterization, antimicrobial studies, and molecular docking studies of transition metal complexes formed from a benzothiazole-based azo ligand. Bulletin of the Chemical Society of Ethiopia. 2023;37(4):931-44.
13. Saleh M, Reem M, Attitalla IH, Saleh A. Algal Bioremediation: Heavy Metals Removal And Evaluation Of Biological Activities In Sewage Plant. Journal of Survey in Fisheries Sciences. 2023:1355-65.
14. Abd El-Nasser MG, Abdel-Latif SA. Ligational behavior of bidentate nitrogen–oxygen donor 8-quinolinolazodye toward Ni2+ and Zn2+ ions: Preparation, spectral, thermal, experimental, theoretical, and docking studies. Applied Organometallic Chemistry. 2023;37(3):e6998.
15. Bufarwa S, Abdel-Latif S, Bahnasy HB. Spectroscopic, Thermal, and Conductometric Studies of Some (Arylazo) Quinolin-8-Ol and Their Complexes with the Divalent Ions of Mn, Ni, Cu, and Zn. Eur Chem Bull. 2023;12:187-97.
16. Abbass L, Sadeek S, Zordok W, El-Telbany M, El-Shwiniy W. Synthesis, Structure, DFT, and Biological Activity of Metal Complexes of Norfloxacin and Metformin Mixed Ligand. Russian Journal of General Chemistry. 2021;91:1774-82.
17. Abbass LM, Sadeek SA, Zordok WA-a, Aziz MAE-R, El-Attar MS. Mixed ligand 4-hydroxy acetanilide-febuxostat complexes of Co (II),-Ni (II), Cu (II) and Zr (IV): Synthesis, structural characterization, DFT calculations, antibacterial, antioxidant and molecular docking studies. Journal of Molecular Structure. 2024;1308:138115.
18. Abdullah A, Mahmoud R. Study and microbial evaluation of home-made meat meals sold in the markets of the city of Al-Bayda–Libya. Medical and Pharmaceutical Journal. 2024;3(1):35-40.
19. Bufarwa S, El-Seifat R, Binhamad H, Hesien R. Synthesis, characterization, thermal, theoretical studies, antimicrobial, antioxidant activity, superoxide dismutase-like activity and catalase mimetics of metal (II) complexes derived from sugar and Schiff base. Reviews in Inorganic Chemistry. 2024(0).
20. Abbass LM, Sadeek SA, Aziz MAE-R, Zordok WA-a, El-Attar MS. Synthesis of some new nanoparticles mixed metal complexes of febuxostat in presence of 2, 2′-bipyridine: Characterization, DFT, antioxidant and molecular docking activities. Journal of Molecular Liquids. 2023;386:122460.
21. Jarad AJ, Dahi MA, Al-Noor TH, El-ajaily MM, AL-Ayash SR, Abdou A. Synthesis, spectral studies, DFT, biological evaluation, molecular docking and dyeing performance of 1-(4-((2-amino-5-methoxy) diazenyl) phenyl) ethanone complexes with some metallic ions. Journal of Molecular Structure. 2023;1287:135703.
22. Bufarwa SM, El-Seifat RM, Binhamad HA, El Fessi KM. Study of Physicochemical Properties of Produced Water in Hamada Oilfield-Libya.
23. Binhamad HA, El-seifat RM, Hesien RA, Bufarw SM. Synthesis, Characterization (IR, Elemental analysis, Molar Conductivity), and Antibacterial Investigation of Complex produced by the reaction between Co (II) ion with mixed ligands of (Amoxicillin and Salen). Al-Mukhtar J Basic Sci. 2023;21:98-104.
24. El-Barasi NM, Miloud MM, El-ajaily MM, Mohapatra RK, Sarangi AK, Das D, et al. Synthesis, structural investigations and antimicrobial studies of hydrazone based ternary complexes with Cr (III), Fe (III) and La (III) ions. Journal of Saudi Chemical Society. 2020;24(6):492-503.
25. Abbass LM. Investigating the Antioxidant Capacity of Ni (II) Complexes with febuxostat in the presence of 2, 2′-bipyridine and paracetamol. Bulletin of Faculty of Science, Zagazig University. 2024;2024(1):168-81.
26. Khalifa HO, Elmanfe GM, Omar SK, Bofarwa SM. Spectrophotometric determination of Caffeine in Nescafe, Cacao, Cappuccino and Coffee samples collected from some Libyan Markets.

27. Abdel-Latif SA, Mohamed AA. Synthesis, structure, spectroscopic properties and DFT studies on some 7-hydroxy-4-methyl-8-(arylazo)-2H-1-benzopyran-2-one and their complexes with some divalent transition metal ions. Journal of Molecular Structure. 2017;1134:307-18.
28. Ibrahim DM, Abdel-Latif SA. Complexation, spectroscopic, thermal, magnetic and conductimetric studies on some 8-(arylazo) coumarins with divalent transition metal ions. IOSR J Applied Chem. 2013;5:40-50.
29. Abdel-Kader NS, Abdel-Latif SA, El-Ansary AL, Sayed AG. Spectroscopic studies, density functional theory calculations, non-linear optical properties, biological activity of 1-hydroxy-4-((4-(N-(pyrimidin-2-yl) sulfamoyl) phenyl) diazenyl)-2-naphthoic acid and its chelates with Nickel (II), Copper (II), Zinc (II) and Palladium (II) metal ions. Journal of Molecular Structure. 2021;1223:129203.
30. Mohapatra RK, El-ajaily MM, Alassbaly FS, Sarangi AK, Das D, Maihub AA, et al. DFT, anticancer, antioxidant and molecular docking investigations of some ternary Ni (II) complexes with 2-[(E)-[4-(dimethylamino) phenyl] methyleneamino] phenol. Chemical Papers. 2021;75:1005-19.
31. Darweesh AF, Abd El-Fatah NA, Abdel-Latif SA, Abdelhamid IA, HM A. Supplementary Material Synthesis and DFT studies of novel aminoimidazodipyridines using 2-(3H-imidazo [4, 5-b] pyrid-2-yl) acetonitrile as an efficient key precursor. ARKIVOC. 2021;8:S1-S26.
32. Mohapatra RK, Sarangi AK, Azam M, El-ajaily MM, Kudrat-E-Zahan M, Patjoshi SB, et al. Synthesis, structural investigations, DFT, molecular docking and antifungal studies of transition metal complexes with benzothiazole based Schiff base ligands. Journal of Molecular Structure. 2019;1179:65-75.
33. Abu-Dief AM, El-Khatib RM, El-Dabea T, Abdel-Latif SA, Barnawi IO, Aljohani FS, et al. Design, synthesize, physicochemical characterization, nonlinear optical properties structural elucidation, biomedical studies, and DNA interaction of some new mixed ligand complexes incorporating 4, 6-dimethylpyrimidine derivative and imidazole ligand. Applied Organometallic Chemistry. 2024;38(6):e7463.
34. Al-Resayes SI, Laria FY, Miloud MM, El-ajaily MM, El-Barasi NM, Sarangi AK, et al. Synthesis, characterization, biological applications, and molecular docking studies of amino-phenol-derived mixed-ligand complexes with Fe (III), Cr (III), and La (III) ions. Journal of Saudi Chemical Society. 2023;27(3):101622.
35. El-ajaily M, Miloud M, Al-noor T, Mohapatra R, Al-barki N. Antifungal Activity Evaluation of Co (II), Ni (II), Cu (II), Zn (II) and Fe (III) Mixed Ligand Complexes with Different Schiff Bases. 2020.
36. Alassbaly F, Maihub A, Ben-Gweirif S, El-Ajaily M, Al-Noor T. Chelation trends and antibacterial activity of some mixed ligand chelates. Saudi Journal of Pathology and Microbiology. 2016;1(2):29-35.

https://journal.utripoli.edu.ly/index.php/Alqalam/index eISSN 2707-7179

تخليق وتوصيف ونشاط مضاد للميكروبات و نظرية الكثافة الوظيفية والالتحام الجزيئي و ADMET ل 4-كلوروفينيل أزوكينولي-8-أول ومجمعاته المعدنية

نجلاء عبد الجليل[1]، صالح بوفروة[2]، مصطفى بلعيدي[3] , ريم السيفاط [4] , عبد السلام صالح[5] , مرعي العجيلي[6]

[1]الهيئة الليبية للبحث العلمي، البيضاء، ليبيا
[2]قسم الكيمياء، كلية العلوم، جامعة عمر المختار، البيضاء، ليبيا
[3] قسم الكيمياء، قسم البيئة المعملية والتنمية المستدامة، جامعة أحمد زبانة، غليزان-الجزائر.
[4] قسم الموارد الطبيعية وعلوم البيئة، جامعة عمر المختار، البيضاء، ليبيا
[5] قسم صحة الغذاء، جامعة عمر المختار، البيضاء، ليبيا
[6] قسم الكيمياء، كلية العلوم، جامعة بنغازي، بنغازي، ليبيا

المستخلص

في هذه الدراسة، قمنا بإعداد 4-كلوروفينيل أزوكينولين، وهو مشتق من 8-هيدروكسي كينولين، مع أيونات Mn(II)، وCo(II)، وNi(II)، وCu(II)، وZn(II) لتحضير معقدات فلزية. لقد استخدمنا طرقًا فيزيائية وطيفية مختلفة لتوصيف المركب ومعقداته الفلزية، بما في ذلك قياسات الموصلية المولية، وتحليل نقطة الانصهار، والتحليل العنصري، وطيف الامتصاص الإلكتروني، وقياس الطيف الكتلي، وطيف الرنين المغناطيسي، وطيف الأشعة تحت الحمراء، والتحليل الوزني الحراري. تم تأكيد هندسة ثماني السطوح لجميع المعقدات المحضرة. لتقييم النشاط المضاد للميكروبات، قمنا بفحص نوعين من سلالات البكتيريا ونوعين من سلالات الفطريات. لوحظ النشاط المضاد للميكروبات للمركبات المحضرة، ولوحظت الزيادة الأعلى في معقد النحاس. تمت دراسة المركبات حاسوبياً بعد تحسين أطوال الزوايا والروابط باستخدام المجموعات الأساسية LANL2DZ*31-6 \ G (d,p) . أظهرت دراسة الالتحام الجزيئي للمركبات التي تحتوي على بروتين مرض الزهايمر BDT4 نشاطًا كبيرًا في الارتباط بالأحماض الأمينية لمركبات HL وC1 و C2 و C3 و C4 و C5، مع طاقات تقارب -6.4 و -6.9 و -6.9 و -6.7 و -7.2 كيلو كالوري / مول للمركبات على التوالي. لتقييم سلامة المركبات المحضرة في تصميمات الأدوية المختلفة، استخدمنا دراسة ADMET، مما قلل من خطر الفشل في مراحل تصميم الأدوية المتقدمة. أظهرت نتائج ADMET انخفاضًا نسبيًا في عامل السمية والسرطان. ومع ذلك، هناك مؤشرات على وجود خطر أيضي وامتصاص خلوي، مما يتطلب مزيدًا من الدراسة.

الكلمات الدالة.